decay. However, in this case, bias for shorter strands might also reflect the asymmetric structure of the DNA molecule pictured in Fig. 1B. The single-stranded character of a portion of the hybrid might affect both the sensitivity of the DNA to radiochemical damage and the distance of the nucleotides from the site of $^{125}I$ decay.

Decay of each $^{125}I$ appears to result in multiple breaks on each strand. If such lesions do occur, they would still be assayed as just one double-strand break by neutral sucrose gradient analysis, which was the method used in the $^{125}I$-IdU suicide experiments with bacteriophages (*1*) and bacteria (*5*). The nature of the lesion will have important implications for repair.

Our results should aid in the design of $^{125}I$-labeled cytotoxic agents. Although the range of $^{125}I$ damage to DNA extends to 70 Å or more from the site of decay, for maximum efficiency the $^{125}I$ isotope should be located no more than 15 to 20 Å from the double helix. This limited range of damage following $^{125}I$ decay may also prove useful in studying the interaction of DNA with proteins and other ligands that can be labeled with $^{125}I$. The results of these experiments are consistent with the calculated energy deposition of low-energy electrons released in the vicinity of $I^{125}$ decay (*8*).

ROGER F. MARTIN*
WILLIAM A. HASELTINE
*Sidney Farber Cancer Institute, Department of Pathology, Harvard Medical School, Boston, Massachusetts 02115*

### References and Notes

1. R. E. Krisch and C. J. Sauri, *Int. J. Radiat. Biol.* **27**, 553 (1975).
2. R. E. Krisch, F. Krasin, C. J. Sauri, *Curr. Top. Radiat. Res. Q.* **12**, 355 (1977).
3. R. F. Martin, *Int. J. Radiat. Biol.* **32**, 491 (1977).
4. ———, T. R. Bradley, G. S. Hodgson, *Cancer Res.* **39**, 3244 (1979).
5. R. E. Krisch, F. Krasin, C. J. Sauri, *Int. J. Radiat. Biol.* **29**, 37 (1976).
6. H. F. Burki, R. Roots, L. E. Feinendegen, V. P. Bond, *ibid.* **24**, 363 (1973).
7. A. M. Maxam and W. Gilbert, *Methods Enzymol.* **65**, 499 (1980).
8. K. Sastry, personal communication.
9. K. L. Berkner and W. R. Folk, *J. Biol. Chem.* **252**, 3176 (1977).
10. W. A. Haseltine, L. K. Gordon, C. P. Lindan, R. H. Gaftstrom, J. L. Shaper, L. Grossman, *Nature (London)* **285**, 634 (1980).
11. W. A. Haseltine, C. P. Lindan, A. D'Andrea, *Methods Enzymol.* **65**, 235 (1980).
12. L. Johnsrud, *Proc. Natl. Acad. Sci. U.S.A.* **75**, 5314 (1978).
13. We thank K. Sastry for communication of results prior to publication and B. Royer-Pokora for help with the restriction map of the *lac* p-o insert in pLJ3 (Fig. 1). This work was supported by grants CA 25118 and CA 19589 from the National Cancer Institute. R.F.M. was supported in part by a study-leave grant from the Cancer Institute, Melbourne, Australia. W.A.H. is recipient of an American Cancer Society faculty research award.
* Present address: Biological Research Unit, Cancer Institute, 481 Little Lonsdale Street, Melbourne 3000, Victoria, Australia.

2 December 1980; revised 19 March 1981

## Fluctuating Responses at a Central Synapse: *n* of Binomial Fit Predicts Number of Stained Presynaptic Boutons

Abstract. *Binomial predictions provided a better description than the Poisson law of fluctuating unitary inhibitory postsynaptic potentials evoked in the goldfish Mauthner cell by impulses in presynaptic interneurons. The number of terminal boutons established on this target cell by each horseradish peroxidase–filled interneuron corresponded to the value of the binomial parameter* n.

Amplitude fluctuations of chemically mediated postsynaptic potentials evoked by single presynaptic impulses can be described by mathematical relations that share one common assumption, namely that the response is made up of an integral number of equal basic units, called quanta. The number of units released depends on both the total amount capable of responding, $n$, and the average probability, $p$, of release of one unit; then $m$, the mean number of quanta responding to one impulse (mean quantal content), can be expressed by the product $np$. When $p$ is made small, such as at the frog neuromuscular junction bathed in low $Ca^{2+}$, high $Mg^{2+}$ solution, the fluctuations are described by Poisson's law, $p_k = (m^k/k!)\, e^{-m}$, where $k$ is a particular number of units constituting a response (*1*). In this case $n$ is large, and it was thus postulated to represent the population of presynaptic vesicles (*2*). However, it is difficult with this model to give independent meaning to $n$ and $p$. Furthermore, at most junctions studied thus far, especially when pharmacological manipulations were avoided, the binomi-

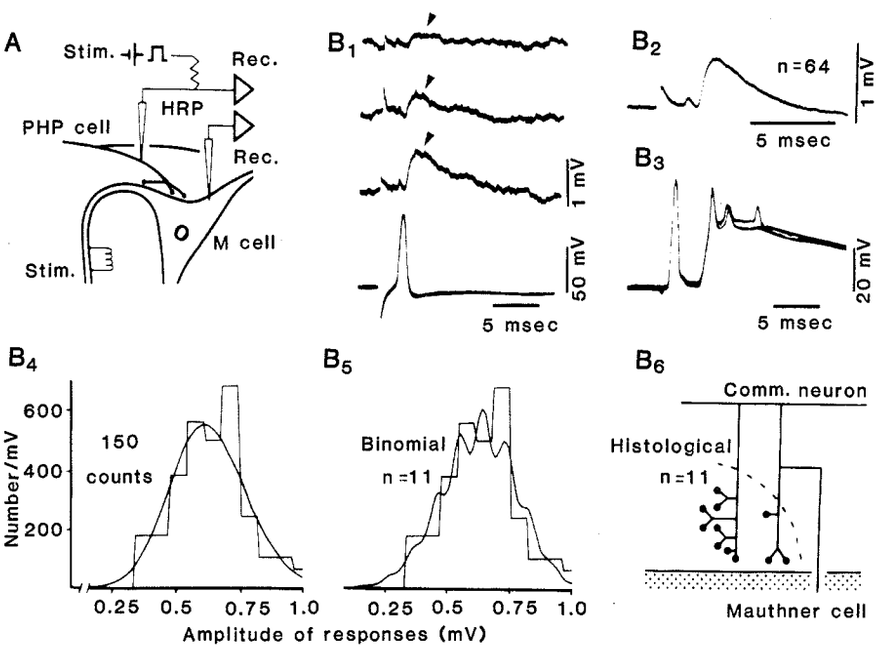


Fig. 1. Evidence for quantal fluctuations of unitary IPSP's. (A) Experimental arrangement used for simultaneous intracellular recordings (*Rec.*) from the M cell and a presynaptic inhibitory interneuron (*PHP cell*), both neurons being identified by their characteristic responses to antidromic stimulation (*Stim.*) of the M axon in the spinal cord. The presynaptic electrode was also used for intracellular stimulation (*Stim.*) and subsequent staining with HRP. ($B_1$ to $B_5$) Properties of depolarizing IPSP's recorded in a $Cl^-$-injected M cell throughout the same experiment. ($B_1$) Variable amplitude of unitary IPSP's (arrows, upper three traces) following single presynaptic impulses directly evoked at a frequency of 1 per second. Only one spike is shown (lower trace). ($B_2$) Computer-averaged unitary IPSP ($N = 64$). ($B_3$) The maximum amplitude IPSP following antidromic activation of the recurrent collateral network was large enough to fire the M cell. ($B_4$ and $B_5$) Comparisons of observed IPSP amplitude variations (stepwise distributions for 150 responses) with best fits (continuous curves) obtained with a Poisson ($B_4$) or binomial ($B_5$) relation. Abscissas show the amplitude of responses evoked by nerve impulses; ordinates, the density of observations expressed as number of occurrences per millivolt. The likelihood criterion was better for the binomial, which yielded a value of 11 for parameter $n$, while $p$ and $q$ were 0.62 and 80 μV, respectively (when derived from the Poisson model, $m$ and $q$ were, respectively, 19 and 30 μV). The binomial prediction satisfied the Kolmogorov test ($P > .05$) but the Poisson did not ($P < .01$). ($B_6$) Schematic representation of the reconstructed presynaptic cell's terminals in relation to the M cell body (shaded area) and its axon cap (dashed line). This cell, which was a commissural (*Comm.*) neuron, established 11 synaptic boutons, represented by closed circles.


0036-8075/81/0821-0898$01.00/0  

al equation, $p_k = \binom{n}{k} p^k (1 - p)^{n-k}$, has provided a more adequate description of the observed amplitude variations (*3*). This expression, of which the Poisson is an extreme case, is often more difficult to apply, especially in the central nervous system, because knowledge of $m$ alone is insufficient for determining $p_k$.

Use of the binomial relation to derive $n$ and $p$ would provide an opportunity to determine possible relations between these parameters and identifiable structural components of presynaptic neurons. Numerous attempts to provide such correlates have been unsatisfactory because they have been inferential, relying on comparisons of physiological and morphological data collected separately. The only conclusion thus far reached, at both the invertebrate neuromuscular junction (*4*) and a central vertebrate synapse (*5*), is that $n$ is much less than the total number of available vesicles, and might be related to the density of presynaptic release sites (*6*), those being poorly defined histologically.

The study we report here was concerned with the characteristics of transmitter release at inhibitory synapses on the goldfish Mauthner (M) cell. This system allows simultaneous recordings from single pre- and postsynaptic neurons, statistical treatment of fluctuating postsynaptic potentials (*7*), and histological reconstruction of the intracellularly stained presynaptic inhibitory cells (*8*). We found that when uncertainty introduced by background noise was minimized, a binomial model provided the best description of the observed fluctuations; more important, there was a one-to-one correspondence between the basic unit $n$, as determined with the binomial fit, and the number of presynaptic boutons. That is, the quantal unit at this central junction is defined by the amount of transmitter released by one bouton.

Experiments were performed on goldfish (*Carassius auratus*) by techniques illustrated in Fig. 1A and described previously (*9, 10*). Recordings from the M cell soma were made with KCl-filled microelectrodes in order to convert inhibitory postsynaptic potentials (IPSP's) into depolarizing responses. In each preparation one cell, belonging to either the M cell's collateral network or a class of commissural vestibular interneurons, was identified by the presence of a passive hyperpolarizing potential (PHP) (*10*) and was impaled with a microelectrode filled with horseradish peroxidase (HRP) for intracellular stimulation, evoking presynaptic impulses at frequencies less than 1 per second, and for dye injection. Techniques for serially reconstructing the interneurons and delimiting the counterstained M cell and for electron microscopy have been described (*8, 11*). The response fluctuations (sample size, 100 to 300) were analyzed with a program developed for a CII Mitra 15 computer.

Figure 1, $B_1$ to $B_6$, illustrates the results of a typical experiment, in which unitary IPSP's were evoked by single presynaptic spikes ($B_1$). In this case the mean IPSP amplitude ($B_2$) was 0.61 mV, that is, about 2.2 percent of the full-sized collateral IPSP ($B_3$), which is a measure of the driving force for $Cl^-$. Overall, the mean IPSP's ranged from 1 to 7 percent of the collateral IPSP (mean, 3.75 percent; standard deviation, ± 2.21; $N$ = 14), indicating that corrections for nonlinear summation of quantal components were not necessary (*12*).

The responses were analyzed statistically, using a model where fluctuations in both evoked IPSP's and background noise summated algebraically according to $X = qK + B$, where $X$ is the observed random variable, $q$ the elementary or quantum size, $K$ the Poisson or binomial variable, and $B$ the noise process. Assuming that the numbers, $k$, of quanta released add algebraically, the amplitude of an individual response, $x$, is determined by $x = qk + b$, where $b$ is the noise contribution at that time. As in other cases (*13*), the noise could be approximated as a white (uncorrelated) Gaussian process (*14*) with a constant variance, $\sigma^2$, which was obtained from direct measurements of spontaneous activity; the value of $\sigma$ ranged from 30 to 90 μV and was generally about 10 percent of the mean evoked response amplitude.

Estimation of parameters defining $K$ on the basis of a sample of $N$ responses is a problem of "constraint deconvolution," requiring definition of a goodness-of-fit criterion, which was chosen as the likelihood criterion, $L$ (*15*). Its definition depended on the statistical characteristics of the background noise; if the observed individual responses had values of $x_i$ with $i = 1, \ldots, N$, then $L$ could be expressed by

$$L(\{x_i\}, n, p, q) = \prod_{i=1}^{N} \sum_{k=0}^{n} \binom{n}{k} \times p^k (1 - p)^{n-k} \times \frac{1}{\sqrt{2\pi}\,\sigma} \exp - \frac{(x_i - qk)^2}{2\sigma^2}$$

for the binomial assumption and

$$L'(\{x_i\}, m, q) = \prod_{i=1}^{N} \sum_{k=0}^{\infty} e^{-m} m^k/k! \times \frac{1}{\sqrt{2\pi}\,\sigma} \exp - \frac{(x_i - qk)^2}{2\sigma^2}$$

for the Poisson assumption. These criteria were maximized by a nonlinear optimization technique (*16*), which yielded the optimal values of the binomial and Poisson parameters and indicated which model provided a better fit. This report includes only cases where the binomial product $np$ did not exceed ~ 7, since above this level several parametric values can be equivalent due to degeneracy (*17*).

The data summarized in Fig. 1, $B_4$ to $B_6$, are representative of the two major results obtained with this analysis. First, the binomial predictions provided a statistically more satisfactory description of the observed fluctuations in IPSP amplitudes than did the Poisson, as shown by a comparison of Fig. 1, $B_4$ and $B_5$. Second, the value of the optimal binomial parameter $n$ was essentially the same (Fig. 1, $B_5$) as the number of stained presynaptic boutons (Fig. 1, $B_6$, and Fig. 2). All synaptic endings of this interneuron could be identified as distinct knobs (Fig. 2, insets), and all necessarily terminated on the M cell, either on its soma or, when distant to it, on dendritic ramifications within the axon cap, as these are their only possible targets in this region (*18*).

Figure 3, $A_1$ to $A_3$, shows that the same results apply to interneurons that also establish synapses on the M cell

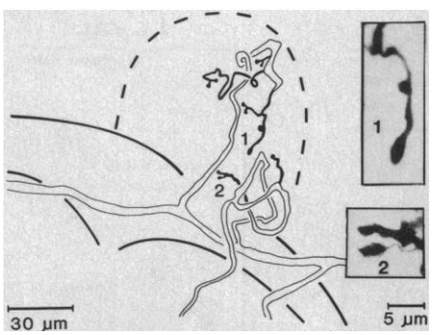


Fig. 2. Camera lucida reconstruction of an HRP-stained inhibitory interneuron presynaptic to the M cell. Same cell as that of Fig. 1; the diagram of Fig. 1, $B_6$, was based on this representation. The M cell soma-dendritic membranes are delimited by bold lines and its axon cap by dashed lines. The primary processes of the presynaptic cell are outlined with thinner double lines and, for simplification, terminal branches and boutons are solid, swellings representing the latter. Eleven boutons were visualized; insets 1 and 2 are light micrographs of the correspondingly labeled terminals. Only those shown in inset 2 impinged directly on the soma; all others, which are somewhat remote from that region, appeared to be in relation to M cell dendrites within the axon cap (see text).

outside the axon cap. Again, the binomial provided the best prediction of the data (Fig. 3, $A_1$) and the number of quantal units determined statistically was equivalent to the total number of synaptic knobs (Fig. 3, $A_3$). This finding is of interest since the terminals are morphologically different, appearing as unmyelinated club endings within the axon cap and small vesicle boutons external to it (*18, 19*). Finally, electron microscopic investigations of about 50 injected terminals, in another series of experiments, confirmed that whatever their localization, all such terminals exhibit the ultrastructural features of transmitting active zones (*20*), as shown for one of them in Fig. 3B. Data from 3 collateral and 11 commissural interneurons are summarized in Fig. 3C, which demonstrates that the equivalence between the *n*'s derived with the two approaches is valid at least for values from 3 to 20. The other binomial parameters were independently distributed, between 0.21 and 0.62 for *p*, and between 0.47 and 2.3 percent of the collateral IPSP for *q*.

In all our experiments the likelihood criterion indicated that the binomial model provided a better description of the data. The Poisson, which was fit with one less degree of freedom, only passed an independent test, the Kolmogorov ($P > .05$), in two of seven cases, and even then at a lower significance level than established for the binomial. The latter satisfied this test in 10 of the 14 experiments, and data from the remaining four were also used for Fig. 3C since the discrepancy between predicted and observed values was localized within a narrow range, presumably because of limited sample size. The large values of *p* are also consistent with a binomial model.

Postsynaptic potentials generated at all synaptic loci could be recorded from the M cell's soma, because (i) even the presynaptic terminals on the primary dendrites are located less than one electrotonic length from the recording site and (ii) the responses generated at distal cap dendrites are also electrotonically close to the cell body, since these processes lie in an extracellular medium of high resistivity (*10*). Thus, any regional variations in quantal size are insufficient to invalidate the model, which provides a reliable indicator of the histological *n*.

Several postsynaptic components have been suggested as physical correlates of *n* (*3*). Our data indicate that at low stimulus frequencies this parameter corresponds to the number of synaptic knobs, each of which contains several distinct presynaptic densities in both stained and unstained material. Our results indicate that each bouton functions as an independent unit, even when in a tight cluster arising from the same terminal. However, whether such a quantal unit releases the contents of one or of a larger, relatively invariant, number of vesicles cannot be specified (*21*). In any case, it seems likely that *n* is a fixed parameter for a given interneuron, as indicated by experiments where stimulus frequency was increased. Acute presynaptic modifications of synaptic efficiency would then be related to changes in the probability of release, *p*, for which this anlysis only provides mean values, and which might be different at each bouton.

HENRI KORN
ANTOINE TRILLER
*INSERM U 3, CHU Pitié-Salpêtrière, 75634 Paris Cedex 13, France*
ALAIN MALLET
*INSERM U 194, CHU Pitié-Salpêtrière, 75634 Paris Cedex 13*
DONALD S. FABER
*Division of Neurobiology, Department of Physiology, State University of New York, Buffalo 14214*

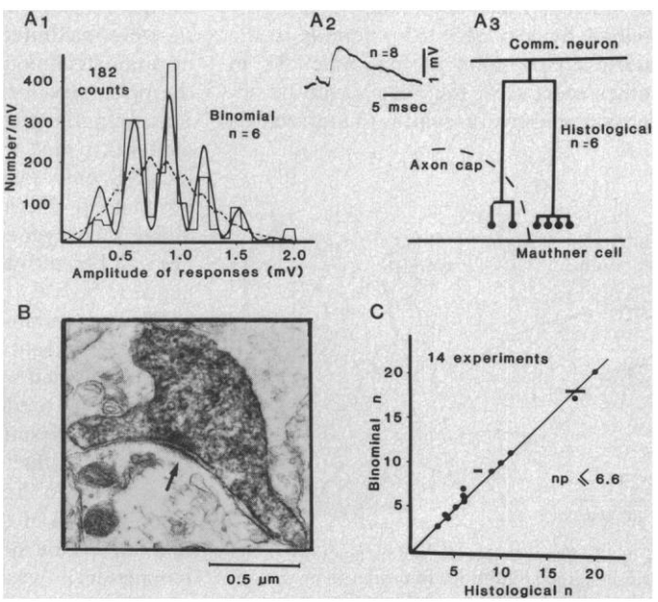


Fig. 3. Evidence that the binomial parameter, *n*, is equivalent to the number of presynaptic endings. ($A_1$ to $A_3$) Correlation of the statistical properties of postsynaptic responses with morphological features of the presynaptic neuron. ($A_1$) Comparison of the observed IPSP amplitude variations (stepwise plot for 182 responses) with best fits obtained with the Poisson (dashed line) and binomial (continuous curve) equations. Same abscissa and ordinate as for Fig. 1, $B_4$ and $B_5$. Only the binomial passed the Kolmogorov test ($P > .05$); its corresponding parameters were $N = 6$, $p = 0.46$, and $q = 310$ μV (the values of *m* and *q* were respectively 5.8 and 153 μV with the Poisson model, the rather small value of the latter accounting for the smooth aspect of the corresponding curve). ($A_2$) Sample computer-averaged unitary IPSP (8 counts); the overall mean amplitude for the 182 trials was 880 μV. ($A_3$) Schematic representation of the terminals established on the M cell by the investigated inhibitory interneuron; of a total of six synaptic boutons (histological *n*), two were within the axon cap and four were outside it. (B) Elecron micrograph, from another preparation, of an HRP-filled bouton established by a PHP-exhibiting collateral interneuron on an M cell cap dendrite. Note the synaptic vesicles, the presynaptic differentiation, and the postsynaptic density (arrow) characterizing chemically transmitting junctions. (C) One-to-one correspondence between the binomial parameter *n* (ordinate) and the number (histological *n*) of synaptic boutons (abscissa), as determined in 14 experiments for which the product *np* was less than or equal to 6.6 (see text). Horizontal bars indicate range of possible histological *n* values in two cases. The solid line is the identity relation. The correlation suggests that for these cells the quantal unit corresponds to the transmitter released by a single bouton.

**References and Notes**

1. J. del Castillo and B. Katz, *J. Physiol. (London)* **124**, 560 (1954).
2. B. Katz. *Nerve, Muscle and Synapse* (McGraw-Hill, New York, 1966).
3. Reviewed in E. M. McLachlan, *Int. Rev. Physiol.* **17**, 49 (1978).
4. A. Wernig, *J. Physiol. (London)* **226**, 761 (1972).
5. M. Kuno and J. N. Weakly, *ibid.* **224**, 287 (1972).
6. R. Zucker, *ibid.* **229**, 787 (1973).
7. H. Korn and D. S. Faber, *Science* **194**, 1166 (1976).
8. H. Korn, A. Triller, D. S. Faber, *Proc. R. Soc. London Ser. B* **202**, 533 (1978).
9. E. J. Furshpan and T. Furukawa, *J. Neurophysiol.* **25**, 732 (1962).
10. D. S. Faber and H. Korn, in *Neurobiology of the Mauthner Cell*, D. S. Faber and H. Korn, Eds. (Raven, New York, 1978), pp. 49–131.
11. A. Triller and H. Korn, *Neurosci. Lett.* **18**, 275 (1980).
12. A. R. Martin, *J. Physiol. (London)* **130**, 114 (1955).
13. F. R. Edwards, S. J. Redman, B. Walmsley, *ibid.* **259**, 665 (1976); A. I. Shapovalov and B. I. Shiriaiev, *ibid.* **306**, 1 (1980).
14. A. H. Jazwinski, *Stochastic Processes and Filtering Theory* (Academic Press, New York, 1970), pp. 81–85.
15. M. G. Kendall and A. Stuart, *The Advanced Theory of Statistics* (Griffin, London, 1961), vol. 2, pp. 1–97.
16. J. A. Nelder and R. Mead, *Comput. J.* 7, 308 (1965); R. O'Neil, *Appl. Stat.* **20**, 338 (1971).
17. M. G. Kendall and A. Stuart, *The Advanced Theory of Statistics* (Griffin, London, ed. 3, 1977), vol. 1, pp. 109–110 and 132.
18. Y. Nakajima, *J. Comp. Neurol.* **156**, 375 (1974).
19. A. Triller, H. Korn, C. Sotelo, *Neurosci. Lett. Suppl.* **5**, S200 (1980).
20. P. Couteaux and M. Pecot-Dechavassine, *C. R. Acad. Sci. Ser. D* **271**, 2346 (1970).
21. Calculations based on the assumptions that one

vesicle opens 2000 channels, a single channel conductance is 20 pS, and the input resistance of the M cell is 200 kilohms favor the hypothesis that one rather than many vesicles is released by a single impulse at each synaptic bouton (H. Korn, D. S. Faber, A. Mallet, A. Triller, *Neurosci. Abstr.*, in press).

22. Supported in part by INSERM grant C.R.L. 78.5.006.6, a grant from the Caisse Mutuelle des Professions Libérales, NIH grant NS 15335, and an INSERM fellowship to D.S.F. We thank M. Depardieu for preparing the figures and C. Sotelo for providing facilities for electron microscopy.

6 February 1981; revised 19 May 1981

# Hyperkeratosis Induced by Sunlight Degradation Products of the Major Polybrominated Biphenyl in Firemaster

Abstract. *Sunlight photodegradation of 2,2',4,4',5,5'-hexabromobiphenyl, the major component of Firemaster, gave a mixture that produces severe hyperkeratosis of the rabbit ear. This component in its pure state does not cause hyperkeratosis. One or more of the four major photolysis products must be responsible for this activity. A similar photodegradation pattern was observed for 2,2',3,4,4',5,5'-heptabromobiphenyl, the second largest component of Firemaster.*

In 1973 and 1974 more than 10,000 Michigan residents—principally farm families and their neighbors—were exposed to grain, meat, dairy, and poultry products that had been contaminated with a mixture containing polybrominated biphenyls (PBB's). The PBB's eventually were detected in a statistically representative sample of persons who had consumed this contaminated food (*1*).

In 1976 several government agencies funded a collaborative study between the Michigan Department of Public Health and the Center for Disease Control to assess and monitor the PBB exposure levels of various groups and adverse health effects. In addition, the Environmental Sciences Laboratory of Mount Sinai School of Medicine studied health effects among exposed farm populations and among workers at Michigan Chemical Company, formerly a producer of PBB's. These two groups showed a 3 and 13 percent incidence of chloracne, respectively (*2*). Chloracne, an acne-like eruption produced by prolonged exposure to certain halogenated aromatic compounds, may be accompanied by systemic toxicity (*2*). Compounds that cause chloracne also produce hyperkeratosis of the rabbit ear. The sensitivity of the rabbit ear to chloracne-causing compounds was first recognized by Adams *et al.* (*3*). The rabbit ear forms lesions exactly like those observed in human chloracne (*4*) and thus is an excellent model for studies of chemicals with this property (*2, 5*). Many investigators have used the rabbit bioassay to identify chemicals with chloracnegenic potential (*2, 5–10*), and we have used the test to assess hyperkeratotic activity in various chemicals (*11–14*).

In the collaborative study (*15*), the Michigan Department of Public Health and the Center for Disease Control have been monitoring the serum concentrations of 2,2',4,4',5,5'-hexabromobiphenyl (PBB-4), which constitutes approximately 60 percent of the commercial PBB mixture (Firemaster FF-1, lot FH 7042) involved in the Michigan PBB incident. However, this may not be the compound responsible for the toxic effects of Firemaster. We previously reported our attempt to identify the toxic components of Firemaster FF-1 by using purified congeners in the rabbit ear test (*12*). We report here studies on the sunlight degradation of certain PBB congeners, their keratotic effects, and PBB contamination of soil at the former manufacturing site in St. Louis, Michigan.

Table 1. Relative amounts of PBB-4 photolysis products at various intervals and rabbit ear test results. Total dose of reaction mixture per rabbit at each interval was 10 mg. Severe hyperkeratosis (+) consisted of dilation of the hair follicles, marked proliferation of the epithelium, and complete atrophy of the sebaceous glands. Abbrevations: N.R., no reaction; N.T., not tested.

| Exposure time (hours) | Amount of product in mixture (%) | | | | Rabbit ear test results |
|---|---|---|---|---|---|
| | PBB-1 | PBB-1a | PBB-2 | PBB-4 | |
| 0.0 | 0.5 | | | 96.0 | N.R. |
| 1.17 | 2.5 | 0.9 | 2.3 | 93.4 | N.T. |
| 2.34 | 4.2 | 1.1 | 4.4 | 86.0 | N.T. |
| 3.5 | 5.8 | 3.0 | 5.7 | 84.0 | (+) |
| 4.67 | 6.3 | 2.9 | 5.8 | 84.6 | N.T. |
| 5.84 | 7.0 | 3.7 | 5.7 | 76.4 | N.T. |
| 7.0 | 8.1 | 4.3 | 6.6 | 71.3 | N.T. |
| 8.17 | 9.7 | 5.1 | 8.7 | 70.8 | N.T. |
| 9.34 | 10.5 | 6.1 | 8.2 | 69.0 | (+) |
| 12.67 | 12.6 | 7.8 | 10.0 | 61.1 | N.T. |
| 17.7 | 14.7 | 8.7 | 9.2 | 52.5 | N.T. |
| 21.25 | 10.8 | 8.1 | 9.4 | 46.8 | (+) |
| 37.67 | 16.7 | 9.7 | 6.0 | 26.7 | (+) |
| 60.0 | 17.4 | 7.8 | 3.8 | 16.4 | (+) |

The photodegradation of PBB-4 by sunlight was conducted in a large quartz reaction vessel containing 0.3125 g of PBB-4 dissolved in 1500 ml of hexane. Portions were taken from the reaction vessel at various intervals for gas chromatography, gas chromatography–mass spectrometry, and rabbit ear tests. The results of the rabbit ear tests (Table 1) clearly show that although PBB-4 is not hyperkeratotic at the 10-mg dose, a severe reaction is produced if PBB-4 is exposed to sunlight for 3.5 hours. Portions removed from the vessel after 1.17 and 2.34 hours of sunlight were not tested for hyperkeratotic activity; therefore, 3.5 hours is not necessarily the minimum time required to produce severe hyperkeratosis.

Figure 1 shows the probable structures of the major photolysis products of PBB-4 (peaks 1, 1a, and 2) after 9.34 hours in the sunlight. The portion removed from the reaction vessel after 3.5 hours did not contain detectable amounts of peaks a, b, or c. Therefore, one or more of the PBB's represented by peaks 1, 1a, and 2 are probably responsible for the severe hyperkeratosis. Support for the structural assignments for peaks 1 and 2 can be found in earlier studies in which Firemaster was exposed to artificially generated ultraviolet light (*16–20*). In one of these studies (*20*), it was suggested that the major peak in the photolysis mixture (peak 1 in Fig. 1) corresponds to the loss of an *ortho* bromine, giving 2,3',4,4',5-pentabromobiphenyl (PBB-2). This PBB, however, was recently identified in Firemaster and characterized (*21*), and its relative retention time corresponds to peak 2 rather than peak 1. Peak 1 has the same retention time and mass spectrum as 2,2',4,5,5'-pentabromobiphenyl, which has also been identified in Firemaster (*21*).

Robertson *et al.* (*22*) showed that PBB-2 is a mixed phenobarbitone- and 3-methylcholanthrene–type inducer of hepatic microsomal enzymes. Loss of the *ortho* bromine by subsequent photolysis of PBB-2 would give peak 1a (tentatively identified as 3,3',4,4'-tetrabromobiphenyl), which has been reported to be a 3-methylcholanthrene–type inducer (*23*). Our gas chromatography–mass spectrometry data indicate that peak 1a represents a mixture of tetrabromobiphenyl and pentabromobiphenyl rather than pentabromobiphenyl alone, as reported earlier (*20*). Support for the tentative structural assignment of the tetrabromobiphenyl as the 3,3',4,4' congener can be found in the Cadagan coupling reaction between 3,4-dibromoaniline and 1,2-di-



0036-8075/81/0821-0901$01.00/0 